Estimating system parameters from chaotic time series with synchronization optimized by a genetic algorithm

Chao Tao, Yu Zhang, and Jack J. Jiang*
Department of Surgery, Division of Otolaryngology Head and Neck Surgery, University of Wisconsin Medical School, Madison, Wisconsin 53792-7375, USA
(Received 15 May 2006; revised manuscript received 27 April 2007; published 11 July 2007)

A method is proposed to estimate system parameters by optimizing synchronization with a genetic algorithm. This method can effectively find the parameter values of a chaotic system with a rugged parameter landscape. Furthermore, even the parameters of a 200-dimensional coupled-map-lattice spatiotemporal chaotic system can be extracted from a scalar time series. Finally, a Chua's circuit experiment shows the capacity of this method to estimate multiple parameters of real systems.

DOI: 10.1103/PhysRevE.76.016209 PACS number(s): 05.45.Gg, 05.45.Xt, 43.70.+i

Chaos phenomena have been widely found in physical and biological systems, such as Taylor-Couette flow [1], atmosphere [2], coupled nonlinear oscillators [3], coupled-map lattices [4], electronic circuits [5,6], the mammalian heartbeat [7], and human voice [8,9]. The parameters of these systems provide insight into their complex behaviors. However, direct measurement of system parameters is often difficult; the time series of a chaotic system can usually be recorded experimentally. Therefore, estimating system parameters from an observed chaotic scalar time series has become an active topic of research [10–21]. Based on a smooth synchronization error landscape, some dynamic methods [15,16] have been successfully applied to extract the parameters of a low-dimensional system. However, the rugged state error landscape with respect to system parameters, and the extreme complexity and parameter sensitivity of a spatiotemporal chaotic system, could create difficulties when using previous parameter estimation methods. To estimate the parameter of the spatiotemporal system, a recent study had to use complete space-time information of the object [12], which is difficult in practical application. Therefore, it is important to develop parameter estimation methods to overcome these difficulties.

We propose a new parameter estimation scheme by integrating synchronization and genetic algorithm (GA). Chaos synchronization provides a determinate relationship between the system status error and their parameter differences [18,22,23]. Based upon the concept of natural selection and survival of the fittest in Darwinian evolution [24–26], GA provides an artificial evolutionary process to optimize the synchronization. GA has been proven to be robust in global optimization [25], and in forecasting and controlling chaos [19,20,27,28]. The proposed method has the features of both synchronization and GA, it has the ability to cope with chaotic systems with rugged state error landscapes and spatiotemporal chaotic systems with extreme parameter sensitivity.

Let the object dynamical system be

$$\dot{\mathbf{x}} = \mathbf{f}(\mathbf{x};\mathbf{c}), \quad \mathbf{c} \in \mathbf{R}^M, \tag{1}$$

whose parameter vector $\mathbf{c}$ needs to be estimated. Assuming $s=h(\mathbf{x})$ is the time series observed from the object system, a model system is coupled with the object system through s using an appropriate synchronization feedback [22,23],

$$\dot{\mathbf{y}} = \mathbf{f}(\mathbf{y},s;\mathbf{\Gamma}(\mathbf{q})). \tag{2}$$

The operator $\mathbf{\Gamma}$ denotes the GA [24,25], which searches for the fittest model parameters to optimize the synchronization between the object and the model. The search starts with one set of randomly generated individuals $\{\mathbf{q}_i\}$, $i=1,2,\ldots,N_p$ defined in the search space $\mathbf{Q}=[u_1,v_1]\cdots\times[u_m,v_m]\cdots\times[u_M,v_M]\subset\mathbf{R}^M$, where u_m and v_m $(1\le m\le M)$ are the lower and upper limits of the search space. Each individual in the population represents a possible parameter vector for the model system (2). A fitness function, defined as

$$F(\mathbf{q}_i) = (t_2 - t_1) \Big/ \int_{t_1}^{t_2} [s - h(\mathbf{y}(\mathbf{q}_i))]^2 dt, \tag{3}$$

is used to weigh the adaptability of each individual, where $\mathbf{y}(\mathbf{q}_i)$ is the state of the model system with the given parameter set $\mathbf{q}_i$. Ranking selection operations [26] reorder the individuals from the best to the worst, i.e., $F(\mathbf{q}_i)>F(\mathbf{q}_j)$ if $i<j$. The selection probability of the ith individual is $p_i=(1-c_s)^i/\sum_{j=1}^{N_p}(1-c_s)^j$, where $c_s=0.005$ is a constant. The probabilistic recombination operation partially exchanges the information between the i and j individuals as $\mathbf{q}_i^{\text{new}}=\alpha\times\mathbf{q}_i^{\text{old}}+(1-\alpha)\times\mathbf{q}_j^{\text{old}}$ and $\mathbf{q}_j^{\text{new}}=\alpha\times q_j^{\text{old}}+(1-\alpha)\times\mathbf{q}_i^{\text{old}}$, where the parameter α is a random number in the interval $[0,1]$. The probabilistic mutation operation introduces new characteristics into the population, $\mathbf{q}_i^{\text{new}}=\mathbf{q}_i^{\text{old}}+\kappa\mathbf{r}\cdot\mathbf{e}$, where the constant $\kappa<0.1$ and $\mathbf{e}$ is a random vector with $\|\mathbf{e}\|=1$. The element r_m of vector $\mathbf{r}$ is defined as $r_m=v_m-u_m$. In order to avoid obtaining new individuals that are located out of the search space $\mathbf{Q}$, each new individual $\mathbf{q}_i^{\text{new}}$ is examined after the mutation operation. If one $\mathbf{q}_i^{\text{new}}$ is out of the search space, the mutation operation is redone on its corresponding $\mathbf{q}_i^{\text{old}}$ until an appropriate individual within the search space is obtained. Repeating the selection, recombination, and mutation opera-

*jjjiang@wisc.edu

tions on the new generations, the evolutionary steps are iterated until an optimized individual is finally found.

GA produces an artificial evolutionary process that drives the population to evolve toward a higher level of fitness. Ideally the fitness value of the fittest individual in an optimized population approaches infinity indicating the identical synchronization [22,23] between model and object systems ($\mathbf{y} \rightarrow \mathbf{x}$). A fitness value approaching infinity produces the same effect as a synchronization error approaching zero. Identical synchronization can usually be achieved when the model and the object have identical parameters [22,23], i.e., when the fittest individual has the same value as the object parameters. In practical conditions, a zero synchronization error cannot be obtained due to system noise, rounding error, etc. In numerical calculations, we will stop the evolutionary process after the best fitness value reaches a sufficiently high threshold value after a number of generations [27]. The resulting maximum fitness value indicates the minimum synchronization error and the fittest individual value is closest to the object parameters. Consequently, the unknown parameters are estimated after the synchronization between the object and model systems are optimized by GA.

Numerical simulation and the electric circuit experiment were used to test the ability of the proposed method. The Duffing system is a typical mechanical system in a twin-well potential field. Moreover, its fitness landscape is quite rugged. A chaotic time series $s=x_1$ is generated from the Duffing system $\dot{x}_1=x_2$, $\dot{x}_2=-(0.1x_2+x_1+x_1^3)+35\cos(\omega_1 t)+40\sin(\omega_2 t)$, where $\omega_1=1.0$ and $\omega_2=1.4$ are the parameters that need to be estimated. The model system is $\dot{y}_1=y_2+(s-y_1)$, $\dot{y}_2=-(0.1y_2+y_1+y_1^3)+35\cos(q_1 t)+40\sin(q_2 t)$. The object and model systems with random initial conditions are solved using the fourth-order Runge-Kutta method with interval step 0.01π. The time series $s=x_1$ with 5000 points is used in the following parameter estimation. Figure 1(a) presents the landscape of the fitness F. Aside from the global peak ($F \rightarrow \infty$) at $q_1=\omega_1$ and $q_2=\omega_2$, there also exist many local peaks. These local peaks in the rugged landscape prevent a gradient-following method [15,16] from finding the true parameter at the global peak because the hill climber could be trapped on the nearest local peak. Therefore, in order to find the true parameter values at the global peak, the gradient-following method would have to preset at an initial parameter that is sufficiently close to the global solution [13–18].

Five-hundred individuals $\mathbf{q}=\{q_1,q_2\}$ are randomly created within the parameter space, $q_1 \in [0,4]$ and $q_2 \in [0,4]$. Selection, recombination, and mutation operations make the population evolve toward a higher fitness, as shown in Fig. 1(b). After about 130 generations, the maximum fitness is above 10^{14}. The model is synchronized with the object and the fittest individual $\{q_1,q_2\}$ converges at $\{1.0,1.4\}$, as shown in Fig. 1(c). This example shows that the proposed method successfully finds the true parameters on a rugged fitness landscape. Recombination operations allow the information exchange among individuals, while random mutation introduces new characteristics that may produce better solutions, which effectively prevent the individuals from getting trapped on a local peak. Because the proposed method has the advantage of GA, it can finally find globally optimized parameters in a wide and uneven search space.

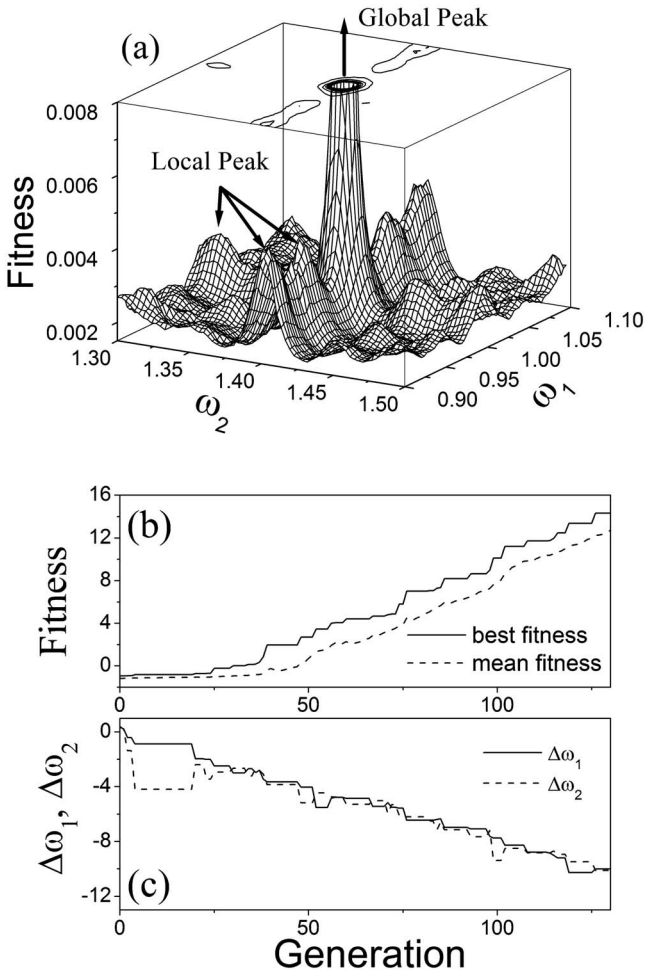

FIG. 1. Parameter estimation of the Duffing system. (a) Fitness landscape. (b) Increase of fitness value during the evolution of population. (c) The fittest individual $\{q_1,q_2\}$ converges at the true parameter $\{\omega_1,\omega_2\}$, where $\Delta\omega_i=\log_{10}(|\omega_i-q_i|)$.

Measurement noise is inevitable in realistic testing conditions. A Gauss random series with zero mean value is added to the chaotic time series x_1 of the Duffing system to represent the measurement noise. Figure 2(a) presents the landscape of the fitness F, where the root mean square of the chaotic time series x_1 is 2.926 and the standard deviation of a Gauss series is 2.0. The height of the global peak ($F \approx 0.007$) is significantly depressed due to the measurement noise. However, its location is not visibly shifted by the noise. We applied the proposed method to estimate the system parameter from the time series that had been polluted by the Gauss noise. Figure 2(b) shows the parameter estimation results. It illustrates that although the measurement noise increases the parameter estimation error, the difference between the estimated parameter and the actual parameter is still very small ($<1.6\times10^{-4}$). This remains true even when the standard deviation of the Gauss noise is increased to 2.0. Therefore, it can be expected that the proposed parameter estimated method could be effective even in the noisy environment.

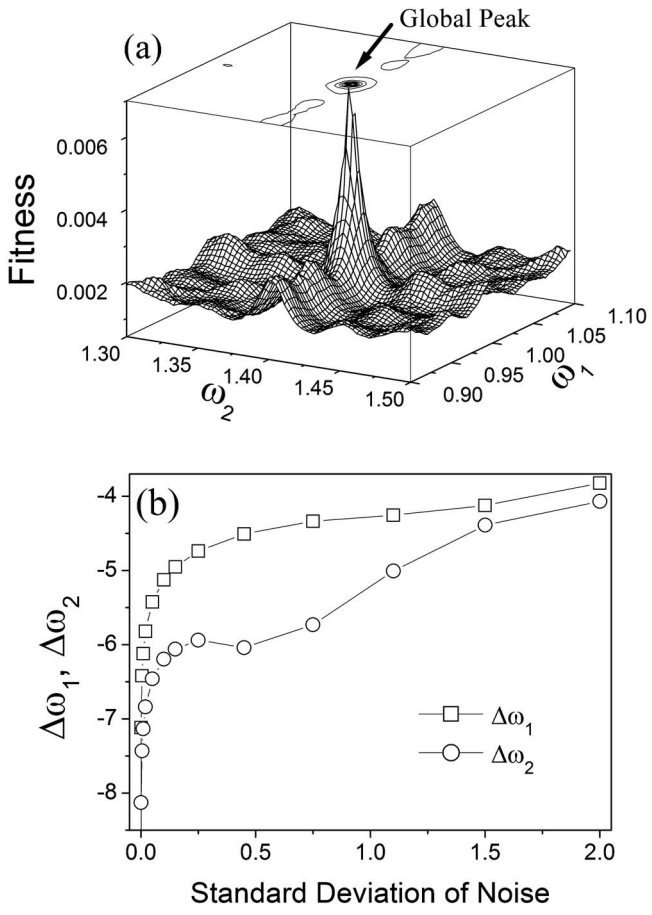

FIG. 2. Parameter estimation of the Duffing system with Gauss noise. (a) Fitness landscape under Gauss noise with the standard deviation of 2.0. (b) Error of the estimated parameter as a function of the standard deviation of Gauss noise, where $\Delta\omega_i = \log_{10}(|\omega_i - q_i|)$.

The L-dimensional coupled map lattice (L-CML) is used in the second example because of its potential application in secure communication [30,31] and wide variety of complex spatiotemporal behaviors, including spatiotemporal chaos [29–31]. In order to improve the time-space complexity, the object CML system combines both a closed loop structure (length R) and an open loop structure (length $L-R$),

$$x_i(n+1) = (1-\varepsilon)f(x_i(n),\mu) + \varepsilon f(x_{i-1}(n),\mu) \quad (1 \le i \le R),$$

$$x_i(n+1) = \left(1-\frac{1}{2}\varepsilon\right)f(x_i(n),\mu) + \frac{1}{2}\varepsilon f(x_{i-1}(n),\mu) \quad (R < i \le L), \tag{4}$$

where $x_0(n) \equiv x_R(n)$, $g(n) = \varepsilon f(x_R(n),\mu)$ is the observed time series of the CML system, the subscript $i = 1,2,\ldots,L$ denotes the lattice site index, and n is the discrete time index. ε is the coupling constant and μ is the parameter of the nonlinear function $f(x,\mu)$, which is the tent map in this study $f(x,\mu) = 2\mu x$ $(0 < x \le 0.5)$ and $f(x,\mu) = 2\mu(1-x)$ $(0.5 < x < 1)$. Letting $L=200$, $R=25$, $\mu=0.785$, and $\varepsilon=0.8$, we generate the signal $g(n)$ from Eq. (4) with random initial conditions. Figure 3(b) shows the complex spatiotemporal pattern of the 200-CML system.

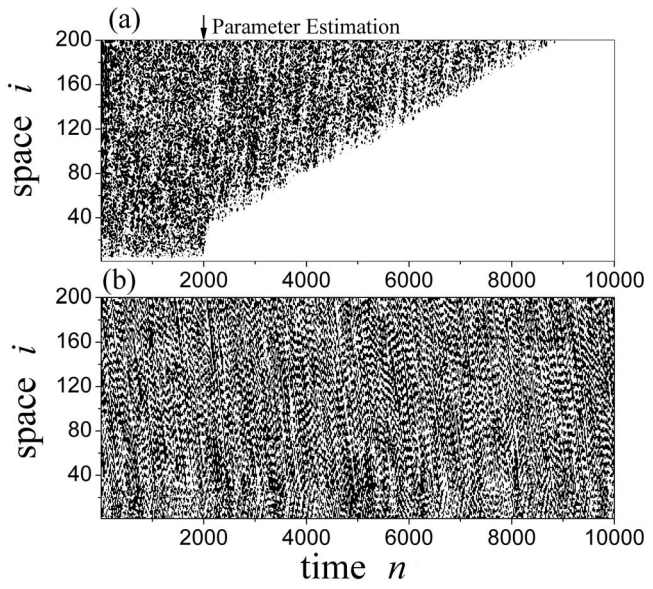

FIG. 3. The spatiotemporal pattern in a 200-CML system. (a) The state error between the object and model. The parameters of the model are $\mu' = 0.78$ and $\varepsilon' = 0.85$ during $n = 1-2000$, but are replaced by the values estimated by the proposed method during $n = 2001-10\,000$. (b) The spatiotemporal chaos in the object with $\mu = 0.785$ and $\varepsilon = 0.8$.

A model is constructed,

$$y_1(n+1) = (1-\varepsilon')f(y_1(n),\mu') + g(n),$$

$$y_i(n+1) = (1-\varepsilon')f(y_i(n),\mu') + \varepsilon' f(y_{i-1}(n),\mu') \quad (2 \le i \le R),$$

$$y_i(n+1) = \left(1-\frac{1}{2}\varepsilon'\right)f(y_i(n),\mu') + \frac{1}{2}\varepsilon f(y_{i-1}(n),\mu') \quad (R < i \le L), \tag{5}$$

and the observed series $g(n)$ with 300 points is used to drive the model system. It has been proven that the model can synchronize with the object for $\mu = \mu'$ and $\varepsilon = \varepsilon'$ [31]. Figure 4(a) presents the fitness landscape in the ε'-μ' parameter space. The fitness landscape of the CML system is also rugged. Moreover, because the error $y_i - x_i$ of CML systems is quite sensitive to parameter differences [31], the global hill around $\varepsilon' = 0.8$ and $\mu' = 0.785$ is rather narrow (in this example, its radius is much smaller than 10^{-5}) [16]. The proposed method finds the parameter value of a CML system in the parameter space $\varepsilon' \in [0.75, 0.95]$ and $\mu' \in [0.7, 0.9]$, which is much wider than the global peak. As shown in Fig. 4(b), the average fitness of the whole population is increased during the artificial evolutionary process. After about 280 generations of evolution, the fitness value was sufficiently high and the fittest individual (ε', μ') converged to (0.8, 0.785). With the estimated parameter [during time $n = 2001-10\,000$ in Fig. 3(a)], the model can be synchronized

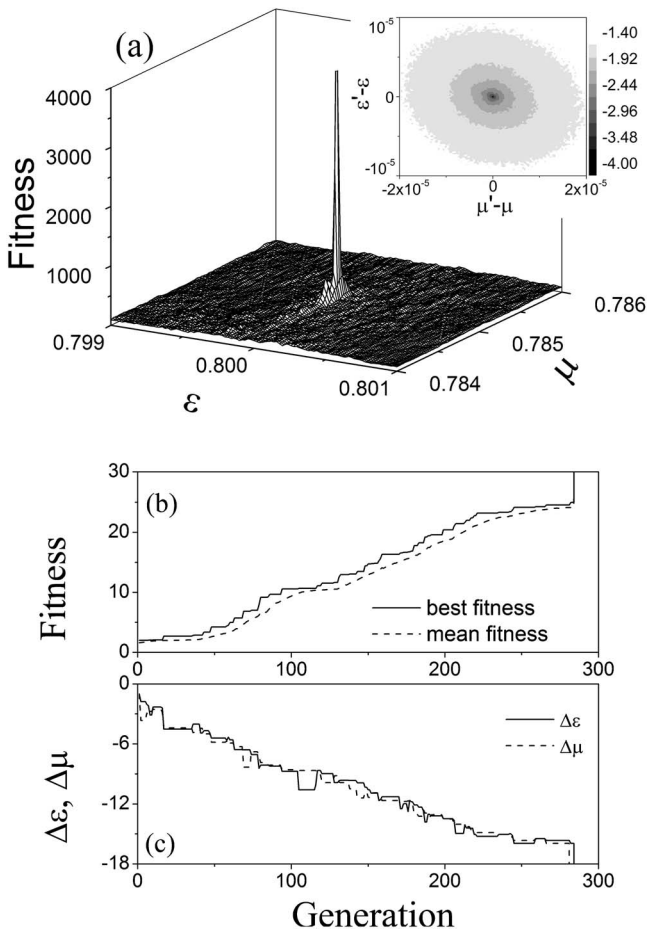

FIG. 4. Parameter estimation of the 200-CML system. (a) Fitness landscape, where the small panel presents the logarithm of the synchronization error between the object and model systems after a gradient-following parameter estimation method is applied. (b) Increase of fitness value during the evolution of population. (c) The fittest individual converges to their true values, where $\Delta\varepsilon = \log_{10}(|\varepsilon - \varepsilon'|)$ and $\Delta\mu = \log_{10}(|\mu - \mu'|)$.

with the object. For the sake of comparison, a gradient-following method [15] is also employed to estimate the parameters of the same CML system. The small panel in Fig. 4(a) presents the convergent range of the gradient-following method, where the gray value represents the logarithm of the synchronization error between the object and model system after the gradient-following parameter estimation method is applied. It is seen that the parameter CML system can be successfully estimated only when the predefined parameter values (ε', μ') are very close to the accurate value $(|\varepsilon' - \varepsilon| \ll 10^{-5}$ and $|\mu' - \mu| \ll 10^{-5})$. The search range of our proposed method $(\varepsilon' \in [0.75, 0.95]$ and $\mu' \in [0.7, 0.9])$ is thousands of times that of the convergent range of the gradient-following method.

This example shows that the proposed method has the potential application of extracting the parameters of a spatiotemporal chaotic system from a scalar time series. The 200-CML system has complex spatiotemporal behavior and system structure. In particular, this spatiotemporal chaotic system is extremely sensitive to parameter perturbation [31].

TABLE I. Parameter values of the Chua circuit.

	Object	Search range	Estimated	Difference (%)
C_1 (nF)	5.13	[0,20]	4.92	−4.09
C_2 (nF)	51.1	[0,200]	50.7	−0.78
G (Ms)	0.675	[0,1]	0.678	+0.44
L (mH)	9.48	[0,20]	9.66	+1.90
R_0 (Ω)	3.46	[0,40]	3.462	+0.06
B_{p1} (V)	−1.59	[−4,0]	−1.544	+2.99
B_{p2} (V)	1.59	[0,4]	1.47	−7.55
m_1 (Ms)	−0.512	[−1,0]	−0.517	−0.98
m_2 (Ms)	−0.511	[−1,0]	−0.536	−4.89
m_{12} (Ms)	−0.835	[−2,0]	−0.840	−0.60

As a result, the global peak in the fitness landscape is extremely narrow. Because of these properties, which make extracting parameters quite difficult [16], the spatiotemporal chaotic system has been utilized to improve the security of a chaotic communication system [31]. In this example, it is found that the proposed method does not need additional assistant systems [18] or control loops [10]. Chaos synchronization maps the parameter difference to the error landscape from just one observable variable. Moreover, GA allows us to optimize the synchronization in such a fitness landscape with extremely narrow global peak. Therefore, the proposed parameter estimation method is still applicable for a highly parameter sensitive spatiotemporal system.

In the third example, we apply the proposed method to estimate the parameters of the Chua's circuit system, based on our experimental setup [32]. Chua's circuit is the simplest electronic circuit that exhibits classic chaos theory behavior. The circuit parameters have been given in the second column of Table I. The time series of V_{C1} and V_{C2} of the Chua's circuit with 10 000 points (20 ms) were recorded through the oscilloscope (Tektronix TDS-460) with the sampling interval 2 μs. Figure 5(a) presents the phase orbits (V_{C1} vs V_{C2}) of the experimental object system. The fluctuation in the attractor is due to the noise in the practical circuit system. To approach the experimental system parameters, we apply the following model system: $C_1\dot{V}'_{C1} = G(V'_{C1} - V'_{C2}) - g(V'_{C1}) + 0.1(V_{C1} - V'_{C1})$, $C_2\dot{V}'_{C2} = G(V'_{C1} - V'_{C2}) + I'_L$, $L\dot{I}'_L = -V'_{C2} - R_0 I'_L$,

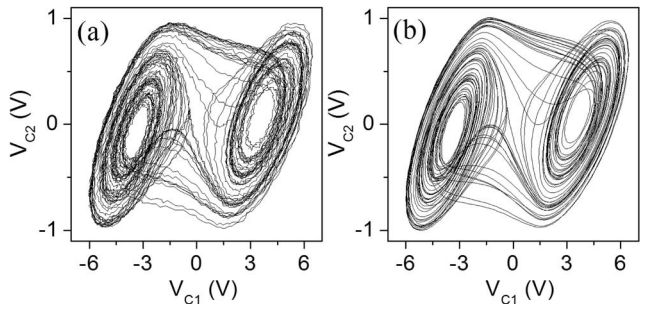

FIG. 5. Chaotic attractor of (a) the Chua's circuit experimental system and (b) the model simulation system with the estimated parameter values given in Table I.

where $g(x)$ is a piecewise-linear function, $g(x)=m_1x+b_1(x<B_{p1})$; $g(x)=m_{12}x(B_{p1}\leq x\leq B_{p2})$; and $g(x)=m_2x+b_2(B_{p2}<x)$ with $b_1=(m_{12}-m_1)B_{P1}$ and $b_2=(m_{12}-m_1)B_{P2}$. Ten independent parameters need to be estimated for a Chua's circuit (column 1, Table I). The fitness function is described as $F=(t_2-t_1)/\int_{t(t1,t2)}(V'_{C1}-V_{C1})^2dt$, where $t_1=2$ ms and $t_2=20$ ms. The proposed method searches for the Chua's circuit parameter values within a wide parameter range (column 3, Table I). The optimized individual is obtained after 200 generations of evolution. The estimated values (column 4, Table I) are close to the measured circuit parameter values. The difference between them may be associated with the measurement error and environmental noise. With the estimated parameter values, the chaotic attractor of the model [Fig. 5(b)] is similar to the object, the Chua's circuit [Fig. 5(a)].

In summary, we propose a method to estimate system parameters from a time series by optimizing synchronization with a genetic algorithm. It is demonstrated that this method can effectively find the actual parameter value from a rugged fitness landscape, even with strong measurement noise. The simulation on a 200-CML system shows that this method can extract the actual parameter from the time series of a single observation even for a complex spatiotemporal chaotic system. Moreover, the search space of our method is much larger in comparison with the gradient-following method. The successful application on a chaotic circuit experiment shows its potential value in extracting real system parameters. To estimate the unknown system parameters of a known system equation from the observed time series has potential application in many practical situations, for example, the secure communication system [22] and vocal-fold system [18]. The function forms of these systems are open or have been built by the previous studies. However, their system parameters are unknown. Extracting the parameters of these systems from the recorded time series could help decode secure communication or provide valuable physiological and pathological information on the vocal fold. It is expected that the proposed parameter estimation method can be applied in these practical situations, which will be interesting for our future work.

This study was supported by NIH Grant Nos. 1-RO1DC006019 and 1-RO1DC05522 from the National Institute of Deafness and other Communication Disorders.

[1] A. Aitta, G. Ahlers, and D. S. Cannell, Phys. Rev. Lett. **54**, 673 (1985).
[2] D. J. Patil, B. R. Hunt, E. Kalnay, J. A. Yorke, and E. Ott, Phys. Rev. Lett. **86**, 5878 (2001).
[3] R. Van Buskirk and C. Jeffries, Phys. Rev. A **31**, 3332 (1985).
[4] T. Bohr and O. B. Christensen, Phys. Rev. Lett. **63**, 2161 (1989).
[5] D. D'Humieres, M. R. Beasley, B. A. Huberman, and A. Libchaber, Phys. Rev. A **26**, 3483 (1982).
[6] A. Cumming and Paul S. Linsay, Phys. Rev. Lett. **60**, 2719 (1988).
[7] C. S. Poon and C. K. Merrill, Nature (London) **389**, 492 (1997).
[8] J. J. Jiang, Y. Zhang, and C. McGilligan, J. Voice **20**, 1 (2006).
[9] Y. Zhang and J. J. Jiang, Phys. Rev. E **72**, 035201(R) (2005).
[10] G. Gouesbet, Phys. Rev. A **44**, 6264 (1991).
[11] B. P. Bezruchko and D. A. Smirnov, Phys. Rev. E **63**, 016207 (2001).
[12] A. Ghosh, V. R. Kumar, and B. D. Kulkarni, Phys. Rev. E **64**, 056222 (2001).
[13] A. Maybhate and R. E. Amritkar, Phys. Rev. E **61**, 6461 (2000).
[14] U. Parlitz, Phys. Rev. Lett. **76**, 1232 (1996).
[15] U. Parlitz, L. Junge, and L. Kocarev, Phys. Rev. E **54**, 6253 (1996).
[16] C. Tao and G. H. Du, Phys. Lett. A **311**, 158 (2003).
[17] C. Tao *et al.*, Phys. Lett. A **332**, 197 (2004).
[18] C. Tao, Y. Zhang, G. Du, and J. J. Jiang, Phys. Rev. E **69**, 036204 (2004).
[19] G. G. Szpiro, Phys. Rev. E **55**, 2557 (1997).
[20] B. A. McKinney, J. E. Crowe, H. U. Voss, P. S. Crooke, N. Barney, and J. H. Moore, Phys. Rev. E **73**, 021912 (2006).
[21] R. Hegger, M. J. Bünner, H. Kantz, and A. Giaquinta, Phys. Rev. Lett. **81**, 558 (1998).
[22] L. M. Pecora and T. L. Carroll, Phys. Rev. Lett. **64**, 821 (1990).
[23] L. Kocarev and U. Parlitz, Phys. Rev. Lett. **74**, 5028 (1995).
[24] D. E. Goldberg, *Genetic Algorithms in Search, Optimization, and Machine Learning* (Addison-Wesley, New York, 1989).
[25] Z. Michalewicz, *Genetic Algorithms + Data Structures =Evolution Programs* (Springer, New York, 1992).
[26] T. C. Fogarty, *Lecture Notes in Computer Science* (Springer, Berlin, 1994).
[27] C. López, A. Álvarez, and E. Hernández-García, Phys. Rev. Lett. **85**, 2300 (2000).
[28] C. Y. Soong, W. T. Huang, F. P. Lin, and P. Y. Tzeng, Phys. Rev. E **70**, 016211 (2004).
[29] F. H. Willeboordse and K. Kaneko, Phys. Rev. Lett. **73**, 533 (1994).
[30] G. Hu, J. Xiao, J. Yang, F. Xie, and Z. Qu, Phys. Rev. E **56**, 2738 (1997).
[31] Y. Zhang, M. Dai, Y. Hua, W. Ni, and G. Du, Phys. Rev. E **58**, 3022 (1998).
[32] Y. Zhang, G. H. Du, and J. J. Jiang, Int. J. Bifurcation Chaos Appl. Sci. Eng. **11**, 2233 (2001).